Nitrogen gas propagation in a liquid helium cooled vacuum tube following a sudden vacuum loss

R C Dhuley[1,2] **and S W Van Sciver**[1,2]

[1] Mechanical Engineering Department, FAMU-FSU College of Engineering, Tallahassee, FL 32310, US
[2] National High Magnetic Field Laboratory, Tallahassee, FL 32310, US

E-mail: rd11d@my.fsu.edu, vnsciver@magnet.fsu.edu

Abstract. We present experimental measurements and analysis of propagation of the nitrogen gas that was vented to a high vacuum tube immersed in liquid helium (LHe). The scenario resembles accidental venting of atmospheric air to a SRF beam-line and was investigated to understand how the in-flowing air would propagate in such geometry. The gas front propagation speed in the tube was measured using pressure probes and thermometers installed at regular intervals over the tube length. The experimental data show the front speed to decrease along the vacuum tube. The empirical and analytical models developed to characterize the front deceleration are summarized.

1. Introduction

Superconducting radio frequency (SRF) cavities in linear accelerators (LINACs) are operated with high vacuum on their inside, while being immersed in a bath of liquid helium (LHe). A string of these cavities housed in a cryomodule forms a long LHe cooled vacuum channel. The accelerator can disrupt catastrophically if the LHe cooled cavity accidentally loses its vacuum to the surrounding atmospheric air. An accidental rupture at a cryomodule interconnect will provide the warm air (≈295 K) a clear path to enter the cavity space. The air will condense/solidify and rapidly deposit heat (≈500 kJ/kg) to the LHe cooled cavity walls. This heat will ultimately transfer to the adjacent LHe coolant, which due to its low enthalpy of vaporization, can violently boil and cause excessive pressure build-up in the cryomodule. Notable experiments to measure the LHe heat load [1, 2] have reported values ranging from 14 kW/m^2 to 23 kW/m^2 with uncertainty as large as 50%. Accurate measurement of the LHe heat load is complicated due to the large length to cross-section ratio of the cavity string. In such a configuration, the air will propagate down the vacuum channel and will condense on the cavity string section that continuously lengthens with the advancing air front. The result will be a longitudinally distributed heat load on the LHe bath from a surface area whose rate of increase will be determined by the speed of air front propagation.

The propagation speed will also determine how quickly a certain length of the beam-line will contaminate. A safety device installed to inhibit the beam-line contamination beyond this length must actuate (close) before the front gets to the device location. The propagation speed thus dictates the device actuation time. Dalesandro *et al.* [3] investigated the longitudinal propagation along a scaled SRF cavity string and observed the air front speed to decrease along the vacuum channel. This deceleration is significant particularly in the case of a real SRF beam-line. A decelerating front will take more time

than a constant speed front to travel from a ruptured interconnect to the location where the front can be arrested. The safety device installed to arrest the front will then have more time to actuate.

This paper reviews the results of our empirical and analytical modeling efforts to charaterize the front propagation. The loss of vacuum experiments [4] used a LHe cooled copper vacuum tube to which near-atmospheric nitrogen gas was vented. The propagation data obtained from a series of experiments show the front to decelerate with the travel length. On regressing these data, the front speed appears to decrease nearly exponentially with the travel length [5]. The analytical model explains why the front decelerates and when supplemented with condensation heat transfer analysis [6], offers support to the observed exponential decay [7].

2. Experimental setup

To study the propagation, we developed an experimental setup that in a simplistic way, resembles the accelerator cavity string layout. The schematic in figure 1 shows the general characteristics of the setup. In this setup, an evacuated copper tube (1.5 m long, 38 mm outer diameter, and 3 mm thick) is immersed in a large bath of LHe. The tube vacuum is isolated from a gas tank by a solenoid valve (SV). On opening this valve, the nitrogen gas (a substitute for air) in the tank vents rapidly to the cold vacuum tube, thus creating a 'sudden loss-of-vacuum' scenario. The setup is designed to generate near constant mass inflow rate to the tube and is instrumented to record the fast rise in the pressure and temperature of the tube due to gas flooding and condensation. The tube carries along its length pressure probes on the inside and thermometers on the outer wall. Figure 1 depicts four sensor stations spaced equally by 0.5 m (the gas flow after venting is from station 1 to station 4). The sensor arrays measure the gas front arrival times at these stations. The known sensor coordinates and the measured front arrival times yield the front speed. Elaborate details of the experimental setup, the gas front tracking techniques, and the data acquisition capabilities are given in [4, 8].

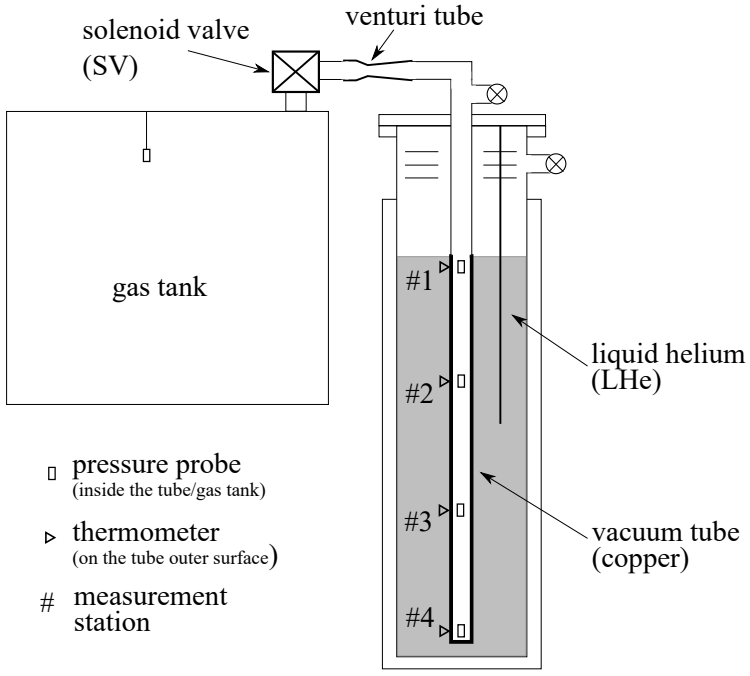

Figure 1. Schematic of the experimental setup

3. Results and discussion

Depicted in figure 2 are the pressure and temperature traces recorded at the four stations on the tube after opening the SV. This experiment used 4.2 K He I as the coolant, the copper tube evacuated to $\approx 10^{-4}$ Pa, and the supply tank containing nitrogen gas at 100 kPa, 295 K. On opening the SV, the gas enters the vacuum tube, propagates down the vacuum space (pressurizes the tube), and condenses on the tube wall (deposits heat and raises the tube temperature). Figure 2(a) shows the pressure rise in the tube. The initial phase of pressurization is due to the forward propagating pressure front, which sets in immediately after the vacuum loss. The pressure rise at station 1 is detected by the pressure probe <5 ms after opening the SV, indicating the arrival of the pressure front at this station. The pressure front then travels down the tube raising the pressure at stations 2, 3, and 4 in their order. The gas in this front condenses on the cold tube wall and warms the tube along its length, again in order from station 1 to station 4. The traces in figure 2(b) clearly show the tube warming up progressively along its length and to above the transition to LHe film boiling temperature [9]. On passing station 4, the gas front encounters the closed end of the tube and is unable to propagate further. The pressure traces in figure 2(a) depict the flow of gas that reflects from the closed end. The gas further flowing in to the tube then pressurizes the tube uniformly over its length (nearly equal pressure at all the stations), until the pressure in the tube equals the supply tank pressure.

The speed of front propagation can be obtained from the front arrival times recorded by the pressure probes as well as by the thermometers. On carefully observing the time axes of figure 2, the propagation of the temperature front in the tube wall (figure 2(b)) appears faster than the propagation of the pressure front in the vacuum space (figure 2(b)). This difference, as elaborated in [5], is due to the thermometers being more responsive in detecting the front arrival than the pressure probes. The front propagation speed in the present study is, therefore, obtained in terms of the arrival times recorded by the thermometers.

The tube wall temperature traces of figure 2(b) also reveal the front deceleration. Clearly, the front takes longer to travel from station 3 to station 4 than it takes from station 2 to station 3, and so on. To study the deceleration further, we installed eight additional thermometers on the vacuum tube and obtained temperature traces at twelve locations over the tube length. This enhancement reduced the spacing between adjacent thermometers from 0.5 m to 0.125 m. Furthermore, we vented nitrogen gas to the vacuum tube at three different mass flow rates by starting with 50 kPa, 100 kPa, and 150 kPa of

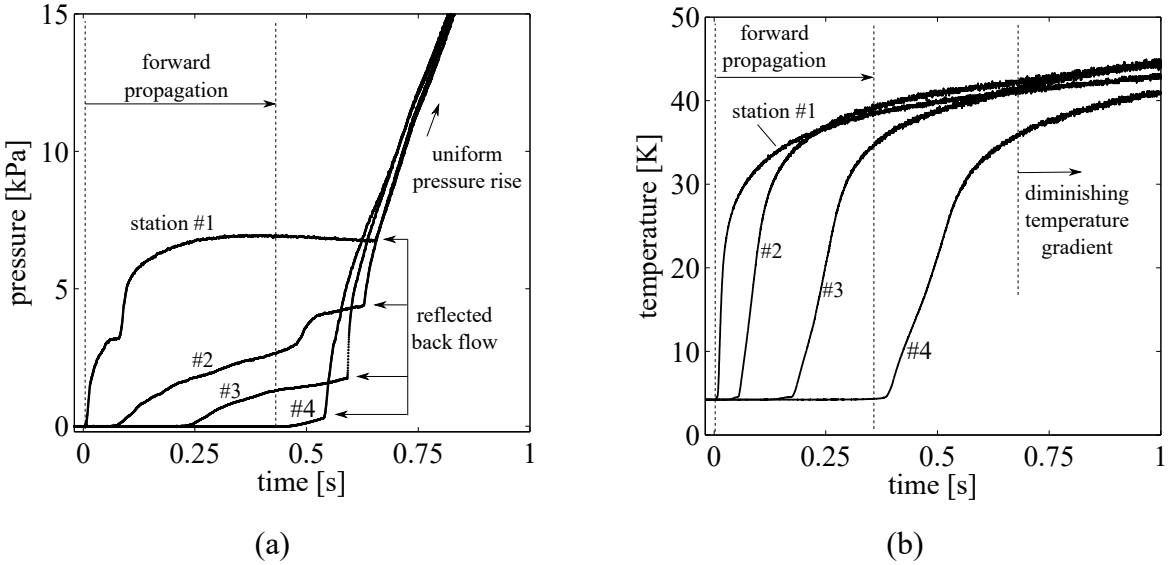

Figure 2. Traces of the tube (a) pressure and (b) wall temperature recorded at the four stations

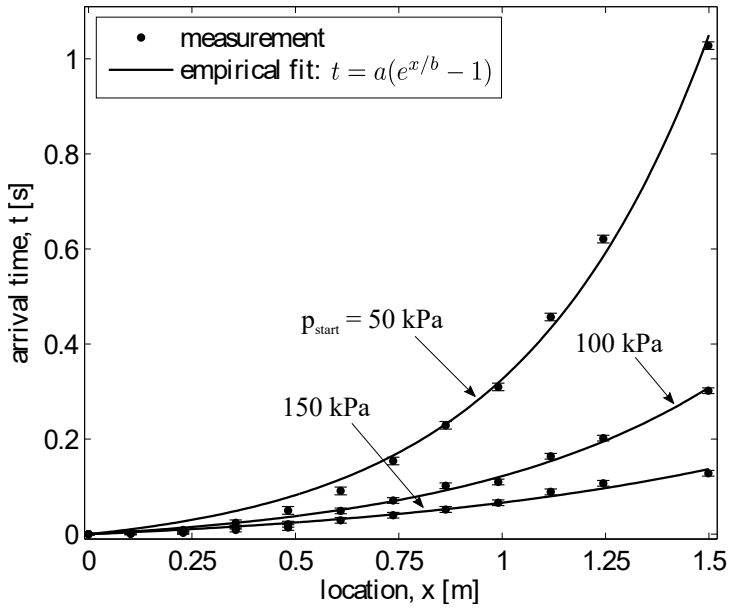

Fit parameters

p_{start} (kPa)	a (s)	b (m)
50	0.041 ± 0.005	0.46 ± 0.02
100	0.031 ± 0.005	0.63 ± 0.04
150	0.035 ± 0.010	0.95 ± 0.15

Figure 3. Gas front arrival times at the twelve thermometer stations fitted with $t = a(e^{x/b} - 1)$. The parameters a and b with their standard errors are listed in the accompanying table.

the gas in the supply tank. The front arrival times at the twelve thermometer stations in this series of experiments are plotted in figure 3 with the locations of the thermometer stations. We defined the arrival time at a location as the time when the temperature at that location exceeds a threshold of ≈10 mK above the initial LHe temperature. The method to define this threshold and to calculate the uncertainty in the arrival times (the error bars) is elaborated upon in [5]. Also plotted in figure 3 are the two-parameter exponential fits $t = a(e^{x/b} - 1)$, which best represent the arrival time (t) *vs.* location (x) data. This non-linear exponential fit ensures that the front is at location $x = 0$ (entrance of the copper tube) at time $t = 0$ (the arrival time at the tube entrance). The fit parameters a and b were obtained by non-linear least squares regression and are tabulated in figure 3 with their standard errors. The fit on taking a derivative with respect to x yields the propagation speed:

$$v = (b/a)e^{-x/b}, \tag{1}$$

suggesting that the front indeed decelerates and its speed decays exponentially along the vacuum tube. The parameter b can be termed as the speed decay length-scale– the travel length over which the speed falls to $1/e$ of its value at $x = 0$. The decay length-scale, as seen in the table of figure 3, is larger for higher starting pressure (higher mass in-flow rate). This outcome is quite intuitive because the gas front arising from a higher mass in-flow rate will travel farther before the front speed falls by a given proportion (for example, $1/e$ of the initial value).

4. Analytical modeling

The analytical model aims to explain the front deceleration. Figure 4 schematically shows a gas front propagating along a vacuum tube in the presence of condensation. The gas enters the vacuum tube at $X = 0$. The gas present over the length $X = x$ condenses on the inner surface of the cold tube. Conservation of mass applied to the gas phase yields the following expression for the front propagation speed:

$$v|_x = \frac{\dot{m}_{in} - \pi D \int_0^x \dot{m}''_{dep}(X,t)\, dX}{(\pi D^2/4)\rho|_x}. \tag{2}$$

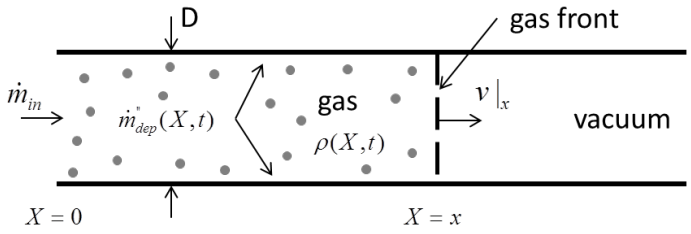

Figure 4. Gas front propagation in a vacuum tube in the presence of condensation

In eq. (2), $\dot{m}_{in}$ is the inlet mass flow rate (taken to be constant with time), $\dot{m}''_{dep}$ is the mass condensation rate per unit surface area (taken to be location and time dependent), D is the tube inner diameter, ρ is the gas density, and $|_x$ denotes the quantities at the gas front. Equation (2) builds by assuming a one-dimensional flow and by taking the mass of gas that remains in the gas phase to be negligible compared to the mass in-flow rate. The steps in deriving eq.(2) are given and the assumptions are justified in [5]. The front deceleration is immediately clear from eq. (2). The propagation speed at x, according to eq. (2), depends on the rate of mass condensation over the length x of the tube. As the front advances, the length x, and consequently the tube surface area on which the gas condenses, will continuously increase. The increasing surface area will remove a larger portion of the constant in-flux of the gas and therefore according to eq. (2), will slow the propagation.

The analytical model of eq. (2) explains the deceleration qualitatively but does not allow to solve for the propagation speed. The main limitation is that $\dot{m}''_{dep}$ over the entire length x is not known and so the integral in eq. (2) cannot be evaluated [5]. However, the model on simplification and when supplemented with $\dot{m}''_{dep}$ at discreet locations along the tube supports the exponential decay.

Assuming that the density of the gas at the front does not significantly change as the front propagates, the derivative of v (eq. (2)) with respect to x gives:

$$(dv/dx)|_x = \frac{-4\dot{m}''_{dep}|_x}{D\rho|_x}. \tag{3}$$

On differentiating with x, the empirical fit of eq.(1) yields:

$$(dv/dx)|_x = (-1/a)e^{-x/b}. \tag{4}$$

If eqs.(3) and (4) are equivalent, then $\dot{m}''_{dep}|_x \propto e^{-x/b}$. This relation implies that the mass deposition rate at the front should decrease exponentially as the front advances in the tube and should have the same decay length-scale, b as that of the front speed. We estimated $\dot{m}''_{dep}$ at the twelve thermometer stations by evaluating the local condensation heat transfer rates at these stations [6] based on the measured temperature data and accounting for the enthalpy of condensation. For the three experiments, the estimated rates of mass deposition $\dot{m}''_{dep}|_x$ *vs.* the location x in the tube are plotted in figure 5 [7]. The error bars represent the uncertainty constituting the measurement and the procedural uncertainty (details presented in [7]). The deposition rate $\dot{m}''_{dep}|_x$ in figure 5 does appear to decay along the tube. We fitted exponential curves of the form $\dot{m}''_{dep}|_x = a''e^{-x/b''}$ to each data set and calculated the fit parameters a'' and b'' by least squares method. The parameter b'' here is the decay length-scale of the deposition rate. The table in figure 5 lists the fit parameters and their standard errors. As elaborated in [7], the mass deposition rates at some stations on the tube (*viz.* stations 1, 4, 6, and 8) are found to carry large error and have been excluded from the fitting routine.

Figure 6 compares the exponential decay length-scales b (based on the arrival times regression) and b'' (obtained from the mass deposition rate analysis). Within the error bars, the decay length-scales obtained

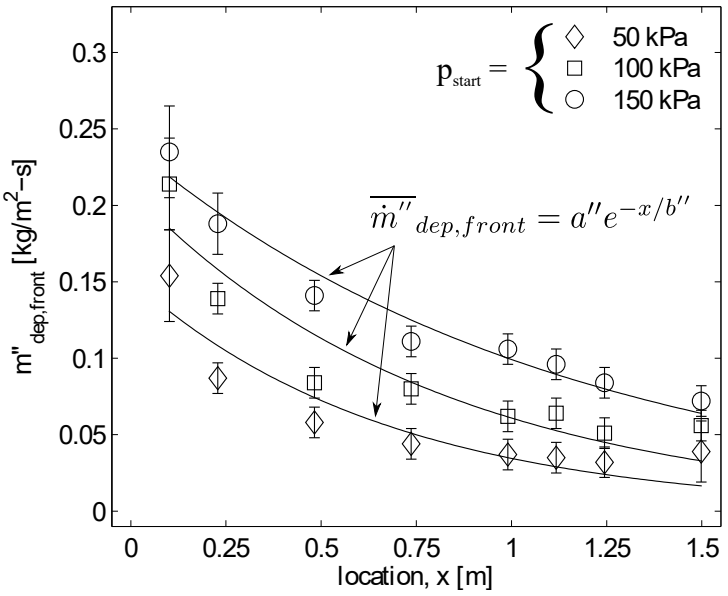

Fit parameters

p_{start} (kPa)	a`` (kg/m^2-s)	b`` (m)
50	0.15 ± 0.02	0.67 ± 0.14
100	0.21 ± 0.02	0.81 ± 0.14
150	0.24 ± 0.01	1.14 ± 0.10

Figure 5. Gas front arrival times at eight thermometer stations fitted with $\dot{m}''_{dep}|_x = a''e^{-x/b''}$. The parameters a'' and b'' with their standard errors are listed in the accompanying table.

from the two independent analyses match reasonably in the trend and in the values. This match further supports the observed exponential decay in the front speed.

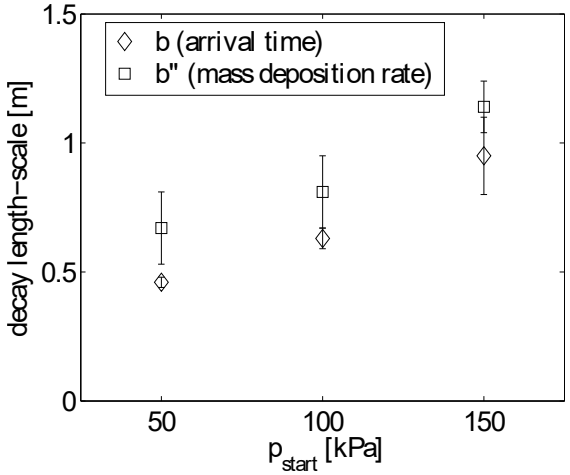

Figure 6. Comparison of the exponential decay length-scales

5. Summary

The experimental measurements show that after sudden venting, a nitrogen gas front propagating in a LHe cooled vacuum channel decelerates along the channel. By relating the front speed to the difference between the mass in-flow rate to the channel and the total mass deposition rate on the channel inner surface, the analytical model provides qualitative support to the front deceleration. The advancing front makes available an increasing condensing surface area, which per unit time will condense more gas from

behind the front. With a constant mass in-flow and increasing mass deposition behind the front, the front speed will decrease with the propagation length.

We regressed the measured front arrival times and found the front speed to decay nearly exponentially with the travel length. The analytical model, on simplification, shows that the spatial derivative of the front speed is proportional to the mass deposition rate near the front. The exponential decay of the front speed results from the exponential decay of the near-front deposition rate. Note from figure 2 that in our experiments, the propagating front was arrested by the closed end of the tube. As a result, we do not know at present if the front will continue to decay exponentially beyond the length of our vacuum tube. Although the near-front mass deposition rate decreases along the tube, the rate is still high enough in the present experiments to onset film boiling in the LHe (see section 3, figure 2(b)). Over longer travel lengths, the deposition rate may fall to values that are insufficient to onset local film boiling in the liquid. The front speed at such lengths may then not decay exponentially. The possibility of a different propagation regime has been discussed in [5].

6. Acknowledgments

Research supported by US Department of Energy grant DE-FG02-96ER40952. Thanks to Dr. Wei Guo and Dr. David Kopriva of Florida State University for several helpful discussions on data analysis. Thanks to the NHMFL CryoLab staff for technical assistance.

7. References

[1] Wiseman M *et al.* 1994 Loss of cavity vacuum experiment at CEBAF *Advances in cryogenic engineering* vol 39 ed Kittel P (New York: Springer-Verlag) pp 997–1003
[2] Boekman T *et al.* 2009 Experimental tests of fault conditions during the cryogenic operation of a XFEL prototype cryomodule *Proc. ICEC22-ICMC2008* vol 22 ed Chang H M (Seoul: Korean Institute of Superconductivity and Cryogenics) pp 723–728
[3] Dalesandro A A, Dhuley R C, Theilacker J C and Van Sciver S W 2014 *AIP Conf. Proc.* **1573** 1822
[4] Dhuley R C and Van Sciver S W 2015 *IEEE Trans. Appl. Supercond.* **25** 9000305
[5] Dhuley R C and Van Sciver S W 2016 *Int. J. Heat Mass Transfer* **96** 573
[6] Dhuley R C and Van Sciver S W 2015 *IOP Conf. Ser.: Mater. Sci. Eng.* **101** 012006
[7] Dhuley R C and Van Sciver S W 2016 *Int. J. Heat Mass Transfer* **98** 728
[8] Dhuley R C and Van Sciver S W 2016 *Cryogenics* **77** 49
[9] Van Sciver S W 2012 *Helium Cryogenics* 2nd ed (New York: Springer)